

Manuscript Number:

Title: Use of cross-borehole DC resistivity tomography to monitor changes in sea ice structure

Article Type: Research Paper

Keywords: sea ice; dc resistivity; microstructure; platelet ice

Corresponding Author: Malcolm Ingham,

Corresponding Author's Institution: Victoria University of Wellington

First Author: Malcolm Ingham

Order of Authors: Malcolm Ingham; Keleigh Jones; Alex Gough; Andrew Mahoney; Pat Langhorne; Tim Haskell

Abstract: Cross-borehole DC resistivity tomography measurements on first-year Antarctic sea ice show a decrease in the horizontal component of resistivity below 0.8 m in depth which is not related to changes in either temperature or brine volume fraction. Microstructural models derived from the resistivity data suggest that this change is related to an increased degree of horizontal connectivity in the brine microstructure of the ice. Comparison of the resistivity data with crystallographic measurements shows that this correlates with a change in ice structure from columnar ice to ice which contains an increasing fraction of platelet ice. It is thus demonstrated that not only can resistivity measurements track the temporal evolution of sea ice microstructure, but are also able to distinguish different ice types. This suggests the dependence of sea ice properties on the distribution of brine inclusions may be studied in-situ through the use of resistivity measurements.



The Editor
Cold Regions Science & Technology

11 November 2011

Dear Sir,

I enclose a manuscript "Use of cross-borehole DC resistivity tomography to monitor changes in sea ice structure" by Jones et al. for consideration for publication in Cold Regions Science and Technology.

At this stage we wish to consider the possibility of Figures 2-6 appearing in colour.

Yours sincerely,

Malcolm Ingham
malcolm.ingham@vuw.ac.nz



SCHOOL OF CHEMICAL & PHYSICAL SCIENCES Te Wānanga Matū

FACULTY OF SCIENCE Te Wāhanga Pūtaiao

PO Box 600, Wellington New Zealand

Phone +64-4-463 5335 Fax +64-4-463 5237 Email scps@vuw.ac.nz Website www.vuw.ac.nz/scps

*Highlights

- We report cross-borehole DC resistivity measurements of Antarctic sea ice
- The depth variation in resistivity does not correlate with changes in temperature
- Structural models show horizontal connectivity of brine pores increases with depth
- This is related to an increased proportion of incorporated platelet ice with depth

1 **Use of cross-borehole DC resistivity tomography to monitor changes**
2 **in sea ice structure**

3

4 K.A. Jones^a, A.J. Gough^b, M. Ingham^{a,*}, A.M. Mahoney^{b,c}, P.J. Langhorne^b, T.G.
5 Haskell^d

6

7 ^aSchool of Chemical & Physical Sciences, Victoria University of Wellington, PO Box
8 600, Wellington 6140, New Zealand

9 ^bDepartment of Physics, University of Otago, PO Box 56, Dunedin 9054, New
10 Zealand

11 ^cGeophysical Institute, University of Alaska Fairbanks, 903 Koyukuk Drive,
12 Fairbanks, AK 99775-7320, USA

13 ^dIndustrial Research Ltd., PO Box 31310, Lower Hutt 5040, New Zealand

14

15 *Corresponding author: Phone +64 4 463 5216, Email Malcolm.Ingham@vuw.ac.nz

16

Abstract

18

19 Cross-borehole DC resistivity tomography measurements on first-year Antarctic sea
20 ice show a decrease in the horizontal component of resistivity below 0.8 m in depth
21 which is not related to changes in either temperature or brine volume fraction.
22 Microstructural models derived from the resistivity data suggest that this change is
23 related to an increased degree of horizontal connectivity in the brine microstructure of
24 the ice. Comparison of the resistivity data with crystallographic measurements shows
25 that this correlates with a change in ice structure from columnar ice to ice which
26 contains an increasing fraction of platelet ice. It is thus demonstrated that not only can
27 resistivity measurements track the temporal evolution of sea ice microstructure, but
28 are also able to distinguish different ice types. This suggests the dependence of sea ice
29 properties on the distribution of brine inclusions may be studied in-situ through the
30 use of resistivity measurements.

31

32

1. Introduction

The bulk properties of sea ice are primarily sensitive to the geometry and connectivity of brine inclusions trapped within the solid ice matrix as the sea ice forms (Weeks, 2010). The size and connectivity of these inclusions vary greatly with temperature and salinity (Light et al., 2003). At low temperatures inclusions tend to be smaller and are isolated between the ice lamellae, whereas as sea ice warms they expand and can ultimately form large connected networks (Eicken et al., 2000). The structure of the brine inclusions is further affected by the growth process of the ice and the type of ice crystals found within the cover (Weissenberger et al., 1992). For instance as sea water begins to freeze ice crystals form, building up a surface slush layer composed of small crystals, called frazil ice. This has a granular structure with random c-axis orientations, with brine inclusions trapped between the crystals. Further growth occurs by grains expanding downwards, with growth favoured along the basal plane of the ice crystals. Geometric selection leads to the formation of vertical columns of ice with their c-axes aligned in the horizontal plane, known as columnar ice. In columnar sea ice brine inclusions and tubes form between the subgrains of the ice matrix with vertical columns aligning with the growth directions of the crystals (Weissenberger et al., 1992; Eicken et al., 2000).

In areas of the Antarctic ocean that lie close to ice shelves, a different growth process of the ice can occur. Ice crystals are found to grow at depth, as water parcels become supercooled through interactions with thick Antarctic ice shelves (Foldvik and Kvinge, 1974; Dieckmann et al., 1986; Williams et al., 1998; Holland and Feltham, 2005). By the end of winter, these crystals accumulate at the base of the sea ice and

expand in place to form a sub-ice platelet layer which can be several meters thick (Serikov, 1963; Smith et al., 2001). These layers are incorporated into the ice cover as it grows downwards (Lange, 1988; Eicken and Lange, 1989; Dempsey et al., 2010) providing a mechanism for increased thickness of sea ice in regions where platelet ice occurs (Crocker and Wadhams, 1989; Purdie et al., 2006; Gough et al., 2011a). The crystal structure of platelet ice is composed of a random distribution of c-axes and large, irregular, bladed crystals (Lange, 1988), so it can be expected that some aspects of the brine microstructure are similarly disordered. The southern end of McMurdo Sound, bounded by McMurdo Ice Shelf (a region of the Ross Ice Shelf), is one area where platelet ice is commonly observed and studied (e.g. Jeffries et al., 1993; Gow et al., 1998; Smith et al., 2001; Jones and Hill, 2001).

Recently Ingham et al. (2008) and Jones et al. (2010) have demonstrated that temporal changes in the anisotropic microstructure of sea ice can be monitored in-situ using cross-borehole DC resistivity tomography. In particular, Jones et al. (2010) presented 3-dimensional numerical models of the horizontal and vertical components of sea ice resistivity derived from a suite of measurements made in first-year landfast sea ice at Barrow, Alaska over the period April-June 2008 as the ice underwent spring warming. These were derived from measurements made using four electrode strings deployed at the corners of a 1 m x 1 m square. Jones et al. (2011b) have subsequently shown how the resistivity data as a function of brine volume fraction may be used to derive models of the sea ice microstructure.

In this paper we present horizontal and vertical resistivity profiles, obtained using the same technique, from McMurdo Sound, Antarctica. We use these data, after the

manner of Jones (2011), to derive basic models of the sea ice microstructure. These suggest a change in brine microstructure with depth. This is confirmed by making crystallographic measurements at the same site, as presented in detail by Gough et al. (2011a). Thus for the first time we demonstrate by direct measurement that changes in brine microstructure detected with electrical measurements are coincident with changes in the crystal structure of the sea ice.

2. Measurements and results

Cross-borehole electrical resistivity measurements were made in McMurdo Sound in first-year sea ice, at a site approximately 10km off the coast of Ross Island, Antarctica (Figure 1). The winter ice growth and ocean conditions at the site are described by Gough et al. (2011a) and Mahoney et al. (2011).

Four 1.8m long electrode strings (Jones et al., 2011a) were installed at the corners of a 1 m square on June 5 2009 when the sea ice was 0.90 m thick. In November, four sets of resistivity data, each comprising approximately 4000 individual measurements, were obtained over a two week period. Salinity data were also obtained from standard measurements on two ice cores. During the two week measurement period the average ice thickness was 2.41 m, meaning that all electrodes were embedded in the sea ice and the ice/water interface was not directly observed. The average snow depth on the ice over this period was 0.16m.

Four cores were also extracted nearby in early October when the ice was 2.00 m thick and transported to a cold laboratory at Scott Base. From these, thin sections were

prepared from depths between 0.50 and 2.00 m. The orientations of crystal c-axes were measured using a universal stage (Langway, 1958).

Sea ice temperature and salinity measurements obtained in the field allow calculation of the brine volume fraction of the ice (Cox and Weeks, 1983). Examples of a series of temperature measurements made over the two week period are shown in Figure 2, corresponding to the dates on which resistivity measurements were made. The temperature in the upper 1 m of the ice showed an increase of 2 to 3 °C over the measurement period. The temperature was high near the surface of the ice then decreased to a minimum at a depth of 10 to 30 cm. Beneath this depth there was a gradual increase in temperature. The two profiles of salinity with depth through the ice were consistent with profiles measured earlier in the winter (Gough et al., 2011b), and were averaged to produce the salinity profile shown in Figure 2. The brine volume fraction of the sea ice, calculated from the salinity profile and the temperature profile at the time, is also shown. The brine volume fraction was below 4% to a depth of ≈ 1.5 m.

Profiles of horizontal (ρ_H) and vertical (ρ_V) resistivity, derived as described by Jones et al. (2010), are shown in Figure 3. The components of the bulk resistivity both show some temporal variation over the measurement period which broadly correlates with the changes in temperature. In particular, lower temperatures between -10 °C and -12 °C in the upper 1 m of the ice correspond to higher values of ρ_H . Over the two week measurement period as temperatures in this region of the ice rose by about 3 °C a corresponding decrease in the bulk horizontal resistivity was observed. Nonetheless, this decrease (from ~ 1000 - 1200 Ωm to 600 - 700 Ωm) is small compared to changes

observed by Jones et al. (2010) in Arctic land-fast sea ice over a nearly two month period in April-June 2008.

The horizontal resistivity profiles display a characteristic shape. Lower surface resistivities may indicate a region of granular ice. Inspection of vertical thin sections revealed a thin layer of frazil ice in the top 0.1 m of the sea ice. Below about 0.9 m there is a significant decrease in resistivity tending to values of the order of 100-200 Ωm at around 1.5 m depth. There is no significant variation in temperature or brine volume fraction to account for these large changes in resistivity. For example, the brine volume fraction (Figure 2) is relatively constant between 0.8 and 1.5 m in depth, and while there is a rise in temperature this is not regarded as large enough to result in significant temperature controlled changes in microstructure which might account for the resistivity variation. Horizontal resistivity profiles from the Arctic (Jones et al. 2010), where the ice is almost entirely columnar in structure, did not show such low values of ρ_H until temperatures in the ice had risen above -4°C .

The profiles of the vertical component of the bulk resistivity are relatively flat between 30 and 60 Ωm . This range is comparable to, but slightly lower, than that observed in the Arctic (Jones et al., 2010). As with the horizontal resistivity profiles, as the ice warmed slightly there was a slight decrease in the resistivity values. An anomalous small peak in ρ_V between 1.2 and 1.3 m depth does not correlate with any obvious feature in the temperature, salinity or brine volume fraction profiles.

In the upper 0.8 m of the ice the coefficient of anisotropy ($\lambda = (\rho_V/\rho_H)^{1/2}$, shown in Figure 6) has values similar to those found throughout the full thickness of columnar

Arctic land-fast ice by Jones et al. (2010). A significant increase in λ , largely due to the observed decrease in ρ_H , occurs below 0.8 m. In Arctic sea ice the only rise in the coefficient of electrical anisotropy occurred at the base of the ice.

Representative horizontal thin sections, cut perpendicular to the direction of growth, are shown in Figure 4. These are photographed through crossed polarising filters. The associated crystal fabric of the sea ice is also displayed in Figure 4. The crystal c-axes (optic axes) lie mainly in the horizontal plane at both 0.60 m and 1.39 m depth, but the distribution becomes more isotropic by 1.60 m. The tendency of the collection of c-axes in the fabric to be clustered in the vertical or horizontal can be summarised by using a crystal anisotropy parameter, in analogy to λ . This is defined as $A = \sum C_V / \sum C_H$, where C_V and C_H are the size of the vertical and horizontal projections of each individual c-axis measurement. $A = 0$ if all c-axes lie in the horizontal plane (a perfect girdle fabric). For the three thin sections shown in Figure 4, $A = 0.23$ and 0.14 for the specimens of columnar ice, and $A = 0.67$ for the platelet ice at 1.60 m.

3. Structural modelling

The observed decrease in horizontal bulk resistivity below about 0.8 m depth and the concomitant rise in λ appear to correlate with a gradual increase in the vertical component of the c-axis distribution. To better understand how this relates to the microstructure of the sea ice we have used the method discussed by Jones et al. (2011b) in which simple models of the microstructure can be derived from the resistivity and brine volume fraction data. Models consist of vertical columns,

horizontal tubes and isolated cubes of brine within a background matrix of pure ice (Figure 5). As the resistivity of the, nearly pure, ice matrix is of the order of $10^7 \Omega\text{m}$ (Petrenko and Whitworth, 1999) continuous vertical and horizontal connections of conductive brine, represented by the columns and tubes, are necessary to yield the observed bulk resistivity values. As is discussed by Jones et al. (2011b), given both ρ_H and ρ_V as a function of brine volume fraction, calculation of the bulk resistivity of the structure shown in Figure 5 in both horizontal and vertical directions can be used to derive the relative dimensions of the brine components in the model (i.e. the width and spacing, a and b , of the vertical columns, the thickness, c , of the horizontal tubes, and the dimension d of the isolated brine pores). The results of such modelling are shown in Figure 5 in which the dimensions are normalised by the value of a at the shallowest depth.

The two week measurement period is sufficiently short that the derived brine structures do not show a clear temporal trend - values for the models obtained for the different dates are closely grouped. This reflects the relatively small variation in the temperature profiles of the ice over the measurement period (Figure 2). The variation in the width of the vertical columns ranges from 1 to 1.4 times the initial width of the vertical columns. Given the constraint inherent in the derivation that the size of the unit cell ($a + b$ as shown in Figure 5) is a constant, the separation between the columns (b) is a mirror image of their width, a . In the upper 0.8 m of the ice the derived width of the horizontal tubes (c) is less than one tenth of the width of the vertical columns. Below this depth, reflecting the observed decrease in ρ_H , there is a steady increase in the thickness of the horizontal tubes. The dimensions of the isolated brine pores (d) are significantly larger than the dimensions a and c of the horizontal

208 tube and vertical column structures. As indicated by Jones et al. (2011b) this can most
209 likely be interpreted as being due to the simple models representing all additional
210 brine outside the vertical and horizontal connections as being contained in a single
211 inclusion. In reality such isolated brine is likely to be spread over a multitude of
212 smaller pore spaces.

213
214 The results shown are similar to those obtained for the microstructure of purely
215 columnar Arctic sea ice (Jones et al., 2011b). However, columnar Arctic sea ice
216 showed very little depth variation in c . The only significant increase in c was observed
217 to occur late in the melt season when the temperature throughout the ice had risen to
218 approximately -2°C . As in the Arctic the derived change in c with depth in the
219 Antarctic data can be interpreted as a transition from grain-boundary conduction to
220 conduction through connected pores. However, there is no indication that this is
221 temperature controlled. It is therefore pertinent to consider if the observed change can
222 be related to a change in the ice structure from near-surface columnar ice to platelet
223 ice at greater depth.

225 4. Discussion

226
227 In the Antarctic, a sub-ice platelet layer can form in the supercooled water beneath the
228 ice cover, creating a tumbled, entwined matrix of platelet crystals. This layer can then
229 become incorporated into the solid ice cover as it grows downwards (Lange, 1988;
230 Leonard et al., 2006; Dempsey et al., 2010). Over the course of the 2009 Antarctic
231 winter a subice platelet layer formed and was incorporated into the sea ice once it
232 reached a thickness of around 1.7 m (Gough et al., 2011a). Analysis of thin sections

obtained from ice cores indicates the following sea ice structure: surface frazil ice above 0.1m, is underlain by aligned columnar ice to a depth of approximately 1.0 m. Below this, small platelets are observed frozen into the columnar ice in increasing proportions to a depth of approximately 1.70 m, where the ice may be characterised as randomly oriented platelet ice.

In sea ice the brine inclusions are trapped between the pure ice crystals. Thus we expect a direct relationship between the distributions of crystal c-axes (as seen in Figure 4) and brine inclusions. In Figure 4(c) we therefore expect to have a greater degree of horizontal connectivity between brine inclusions than is seen in vertically aligned columnar ice of Figures 4(a) and (b). This greater horizontal connectivity should result in a lower horizontal component of bulk resistivity. Thus it seems likely that the observed horizontal resistivity decrease (Figure 3) and the increase in the thickness of the horizontal tubular connections in the structural model (Figure 5), are a result of a change in ice type from columnar ice to platelet ice. At depths above 0.8 m the predominance of columnar ice means that there is little horizontal connectivity between actual brine inclusions and electrical conduction is along grain-boundary films. Beneath this depth, as more platelet ice appears, the randomly orientated ice crystals allow a greater horizontal connectivity of brine pores as indicated by the increase in horizontal tube thickness in the microstructural model (Figure 5).

The likely affect of platelet ice on the bulk vertical resistivity is difficult to predict. Compared to columnar ice, a region of platelet ice might be expected to have somewhat reduced vertical connectivity between brine inclusions. Such a reduction would be reflected in an increased vertical resistivity. As can be seen in Figure 3,

below about 1.2 m depth a slight increase in vertical resistivity is indeed observed. However, beneath this depth the ρ_V profiles also become somewhat more scattered and it is not possible to draw firm conclusions. The significant increase in the coefficient of electrical anisotropy also suggests a change from an anisotropic brine structure in a region of columnar ice to a more isotropic structure in a region of platelet ice.

These suggested changes in structure inferred from the resistivity measurements and modelled brine structure are consistent with the crystallographic analysis of ice core thin sections. For example Figure 4 shows a mostly columnar ice structure at depths of 0.6 m and 1.39 m, with definite platelet ice at 1.60 m depth. This is in agreement with the suggested regions of columnar ice above 0.8 m, followed by a transition region where columnar ice is mixed with small amounts of platelet ice, before reaching a region of mainly platelet ice at the base of the resistivity profiles (see also Gough et al., 2011a). The evidence can be quantified as shown in Figure 6 which shows the variations with depth of both the electrical coefficient of anisotropy (λ) and the crystal fabric anisotropy (A). The electrode strings have an electrode spacing of 0.1 m vertically, and thus have a vertical resolution of around 0.2 m. We have produced a vertical profile of crystal structure which matches the resolution measured by the resistivity probes by calculating $A(z)$ from all c-axis measurements within $z \pm 0.1$ m. Notwithstanding that the crystallographic data are only available beneath 0.5 m depth, it can clearly be seen that the variation in c-axis orientation correlates strongly with λ suggesting that the resistivity measurements have indeed identified the change in ice structure from columnar ice to platelet ice.

5. Conclusions

Previous cross-borehole DC resistivity measurements on sea ice (Ingham et al., 2008; Jones et al., 2010) have demonstrated that the technique is able to monitor evolution of the sea ice microstructure with temperature. Jones (2011) and Jones et al. (2011b) have shown how these data may be interpreted in terms of simple models of the microstructure. In this paper we demonstrate, by direct measurement, that changes in brine microstructure detected with electrical measurements are coincident with changes in the crystal structure of the sea ice. The electrical properties are controlled by the distribution and connectivity of brine within the ice matrix. Using a simple model of brine connectivity to explain our electrical measurements, we show that platelet ice has a higher degree of horizontal connectivity within the brine microstructure than columnar ice. If this higher horizontal connectivity also exists while the ice is more porous during its formation, this has implications for how brine circulates within the sea ice during the formation of platelet ice.

The distribution of platelet ice is strongly related to the prevailing oceanic conditions, and in the Antarctic is related to the presence of supercooled water originating beneath the ice shelves. Resistivity measurements, which can be carried out with little disturbance to the ice, may thus be able to play a role in monitoring and understanding the interaction of ice shelves with the ocean, and their impact upon sea ice formation. The ability to differentiate different types of ice permits the in-situ study of the dependence of a variety of properties of sea ice on the distribution of liquid inclusions within it.

Acknowledgements

This research, which forms part of New Zealand's contribution to the IPY, was funded by the Foundation for Research, Science and Technology and Postgraduate Scholarships from the University of Otago (AJG) and Victoria University of Wellington (KAJ). We are grateful to Brian Staite and the 2009 Scott Base wintering team for support in the field. Peter Stroud and Richard Sparrow helped to construct instruments.

References

- Cox, G. F. N., Weeks, W. F., 1983. Equations for determining the gas and brine volumes in sea-ice samples. *J. Glaciol.*, 29, 306–316.
- Crocker, G. B., Wadhams, P., 1989. Modeling Antarctic fast-ice growth. *J. Glaciol.*, 35(119), 3-8.
- Dempsey, D. E., Langhorne, P. J., Robinson, N. J., Williams, M. J. M., Haskell, T. G., Frew, R. D., 2010. Observation and modelling of platelet ice fabric in McMurdo Sound, Antarctica. *J. Geophys. Res.*, 115, C01007, doi: 10.1029/2008JC005264.
- Dieckmann, G., Rohardt, G., Hellmer, H., Kipfstuhl, J., 1986. The occurrence of ice platelets at 250 m depth near the Filchner ice Shelf and its significance for sea ice biology. *Deep Sea Research Part A. Oceanographic Research Papers*, 33(2), 141-148.

- 333 Eicken, H., Lange, M. A., 1989. Development and properties of sea ice in the coastal
334 regime of the southeastern Weddell Sea. *J. Geophys. Res.*, 94(C6), 8193-8206.
335
- 336 Eicken, H., Bock, C., Wittig, R., Miller, H., Poertner, H. -O., 2000. Magnetic
337 resonance imaging of sea pore fluids: methods and thermal evolution of pore
338 microstructure. *Cold Reg. Sci. Technol.*, 31, 207-225.
339
- 340 Foldvik, A. T., Kvinge, T., 1974. Conditional instability of sea water at freezing
341 point. *Deep Sea Res.*, 21(3), 169-174.
342
- 343 Gough, A. J., Mahoney, A., Langhorne, P. J., Williams, M. J. M., Robinson, N. J.,
344 Haskell, T. G., 2011a. Signatures of supercooling: McMurdo Sound platelet ice. *J.*
345 *Glaciol.* (in press)
346
- 347 Gough, A. J., Mahoney, A., Langhorne, P. J., Williams, M. J. M., Haskell, T. G.,
348 2011b. Sea ice salinity and structure - a winter time series of salinity and its
349 distribution. Submitted to *J. Geophys. Res.*
350
- 351 Gow, A., Ackley, S., Govoni, J., Weeks, W., 1998. Physical and structural properties
352 of land-fast sea ice in McMurdo Sound, Antarctica. *Ant. Res. Ser.*, 74, 355-374.
353
- 354 Holland, P. R., Feltham, D. L., 2005. Frazil dynamics and precipitation in a water
355 column with depth-dependent supercooling. *J. Fluid Mech.*, 530, 101-124.
356

- 357 Ingham, M., Pringle, D., Eicken, H., 2008. Cross-borehole resistivity tomography of
358 sea ice. *Cold Reg. Sci. Technol.*, 52, 263-277, doi: 10.1016/j.coldregions.2007.05.002
359
- 360 Jeffries, M., Weeks, W., Shaw, R., Morris, K., 1993. Structural characteristics of
361 congelation and platelet ice and their role in the development of Antarctic land-fast
362 sea ice. *J. Glaciol.*, 39, 223-238.
363
- 364 Jones, K. A., 2011. Cross-borehole DC resistivity tomography of sea ice: temporal
365 and spatial variations in the anisotropic microstructure. Unpublished PhD Thesis,
366 Victoria University of Wellington, New Zealand.
367
- 368 Jones, K. A., Ingham, M., Pringle, D. J., Eicken, H., 2010. Temporal variations in sea
369 ice resistivity: resolving anisotropic microstructure through cross-borehole dc
370 resistivity tomography. *J. Geophys. Res.*, 115, C11023, doi:10.1029/2009JC006049.
371
- 372 Jones, K.A., Ingham, M., Pringle, D. J., Eicken, H., 2011a. Cross-borehole resistivity
373 tomography of Arctic and Antarctic sea ice. *Annals. Glac.*, 52(57), 161-168.
374
- 375 Jones, K. A., Ingham, M., Eicken, H., 2011b. Modelling the anisotropic brine
376 microstructure in first-year sea ice. Submitted to *J. Geophys. Res.*
377
- 378 Jones, S. J., Hill, B. T., 2001. Structure of sea ice in McMurdo Sound, Antarctica.
379 *Ann. Glaciol.*, 33, 5-12.
380

- 381 Lange, M.A., 1988. Basic properties of Antarctic sea ice as revealed by textural
382 analysis of ice cores. *Ann. Glaciol.*, 10, 95-101.
383
- 384 Langway, C., 1958. Ice fabrics and the universal stage. Tech. Rep. 62, U.S. Army
385 Snow, Ice and Permafrost Research Establishment.
386
- 387 Leonard, G. H., Purdie, C. R., Langhorne, P. J., Haskell, T. G., Williams, M. J. M.,
388 Frew, R. D., 2006. Observations of platelet ice growth and oceanographic conditions
389 during the winter of 2003 in McMurdo Sound Antarctica. *J. Geophys. Res.*, 111,
390 C04012, doi: 10.1029/2005JC002952.
391
- 392 Light, B., Maykut, G. A., Grenfell, T. C., 2003. Effects of temperature on the
393 microstructure of first-year Arctic sea ice. *J. Geophys. Res.*, 108(C2), 3051,
394 doi:10.1029/2001JC000887.
395
- 396 Mahoney, A. M., Gough, A. J., Langhorne, P. J., Robinson, N. J., Stevens, C. L.,
397 Williams, M. J. M., Haskell, T. G., 2011. The seasonal arrival of ice shelf water in
398 coastal Antarctica and its effect on sea ice growth. *J. Geophys. Res.*, in press, doi:
399 10.1029/2011JC007060.
400
- 401 Petrenko, V.F., Whitworth, R. W., 1999. *Physics of ice*. Oxford University Press.
402
- 403 Purdie, C., Langhorne, P. J., Leonard, G., Haskell, T. G., 2006. Growth of first-year
404 landfast Antarctic sea ice determined from winter temperature measurements. *Ann.*
405 *Glaciol.*, 44, 172.

406

407 Serikov, M.I., 1963. Structure of Antarctic sea ice. Sov. Antarctic Exped. Inform.
408 Bull., 39, 13-14.

409

410 Smith, I. J., Langhorne, P.J., Haskell, T. G., Trodahl, H. J., Frew, R., Vennell, M. R.,
411 2001. Platelet ice and the land-fast ice of McMurdo Sound, Antarctica. Ann. Glaciol.,
412 33, 21-27.

413

414 Weeks, W.F., 2010. On Sea Ice. University of Alaska Press, Fairbanks, Alaska.

415

416 Weissenberger, J., Dieckmann, G., Gradinger, R., Spindler, M., 1992. A cast technique
417 to examine and analyze brine pockets and channel structure. Limnology and
418 Oceanography, 37, 179-183.

419

420 Williams, M.J.M., Jenkins, A., Determann, J., 1998. Physical controls on ocean
421 circulation beneath ice shelves revealed by numerical models. Ant. Res. Ser., 75, 285-
422 299.

423

Figure captions

Figure 1: Map showing the location of the field site near Ross Island. Dashed lines show the edge of the multiyear ice cover, the solid black line shows the approximate edge of the McMurdo Ice Shelf. EGT – Erebus Glacier Tongue.

Figure 2: Temperature, salinity and brine volume fraction as a function of depth. Colours on the temperature plot represent different dates: blue – 11/12 November 2009, green – 15/16 November 2009, orange – 19 November 2009, red – 21 November 2009. The dotted line indicates the base of the electrode strings used for the resistivity measurements. The dashed line shows the depth of the ice-water interface at the time of measurement.

Figure 3: Depth dependence of the horizontal and vertical components of sea ice resistivity. Different curves represent results from different dates as in Figure 2.

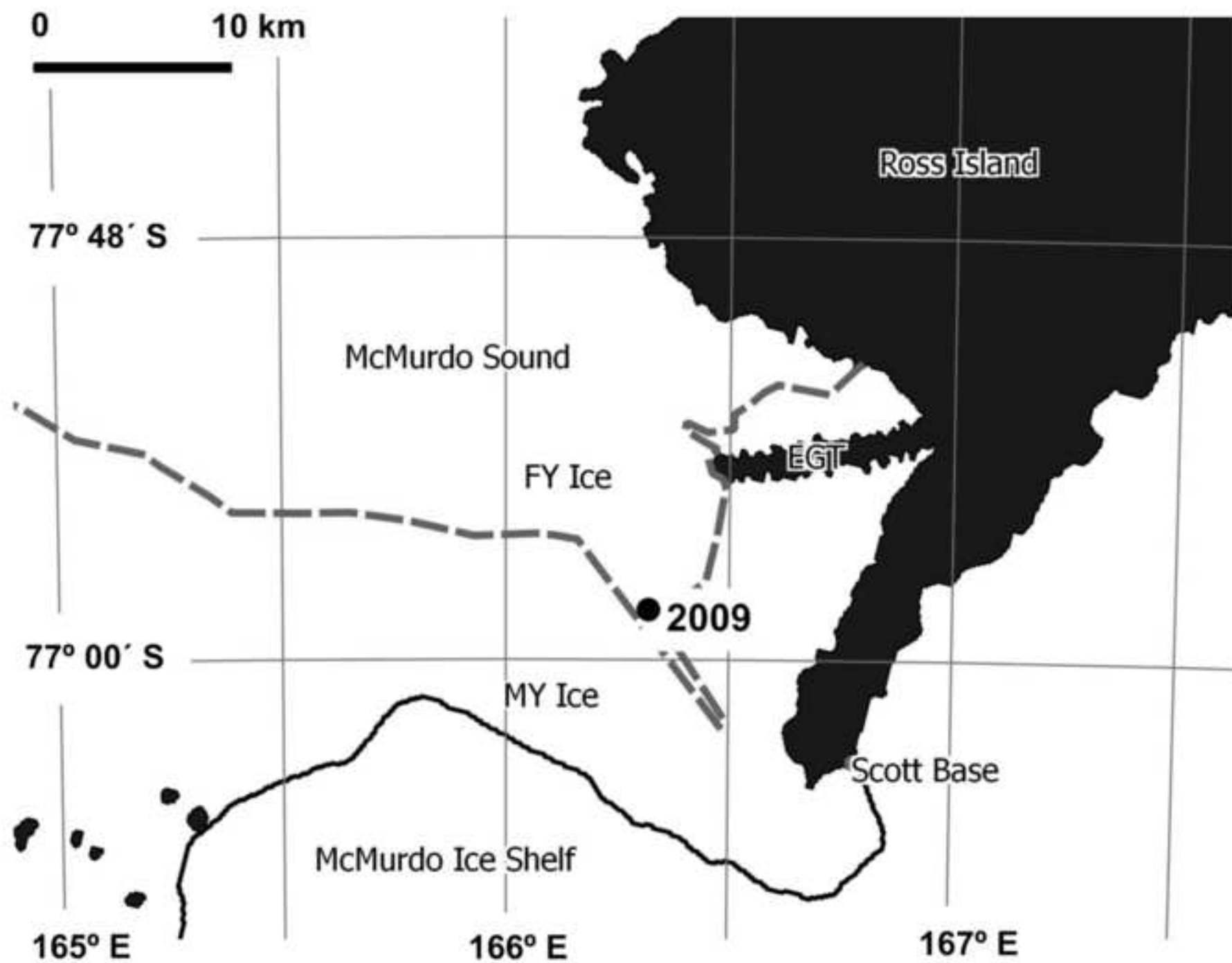
Figure 4: Representative c-axis fabrics and thin sections (90 mm diameter) (a) 0.60 m, (b) 1.39 m and (c) 1.60 m depth in the sea ice. A indicates the fabric anisotropy for each thin section.

Figure 5: Simple structural model of sea ice (consisting of brine inclusions of conductivity σ_2 in an ice matrix of conductivity σ_1) and the derived variations with depth in the ice of parameters a , b , c and d . Where visible, different colours represent results from measurements made on different days as in Figure 2. All dimensions are relative to the smallest value of a on 15/16 November.

449 Figure 6: Electrical and crystallographic anisotropy as a function of depth.

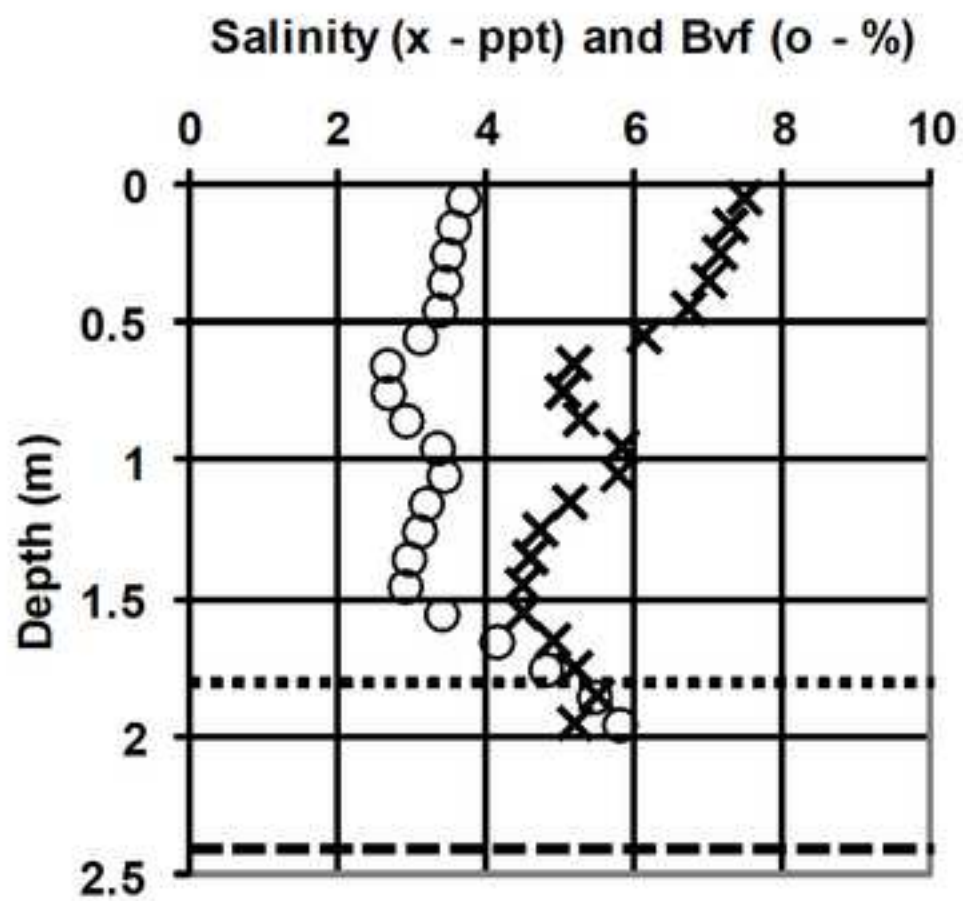
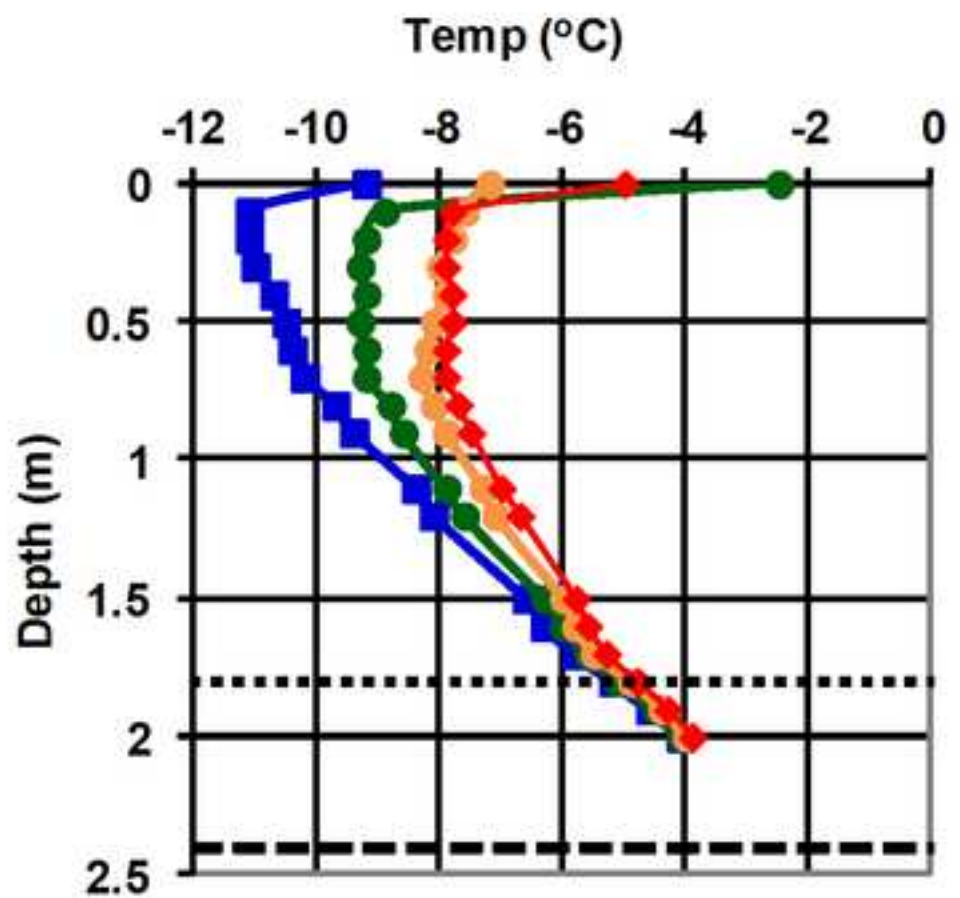
450

Figure(s)
[Click here to download high resolution image](#)



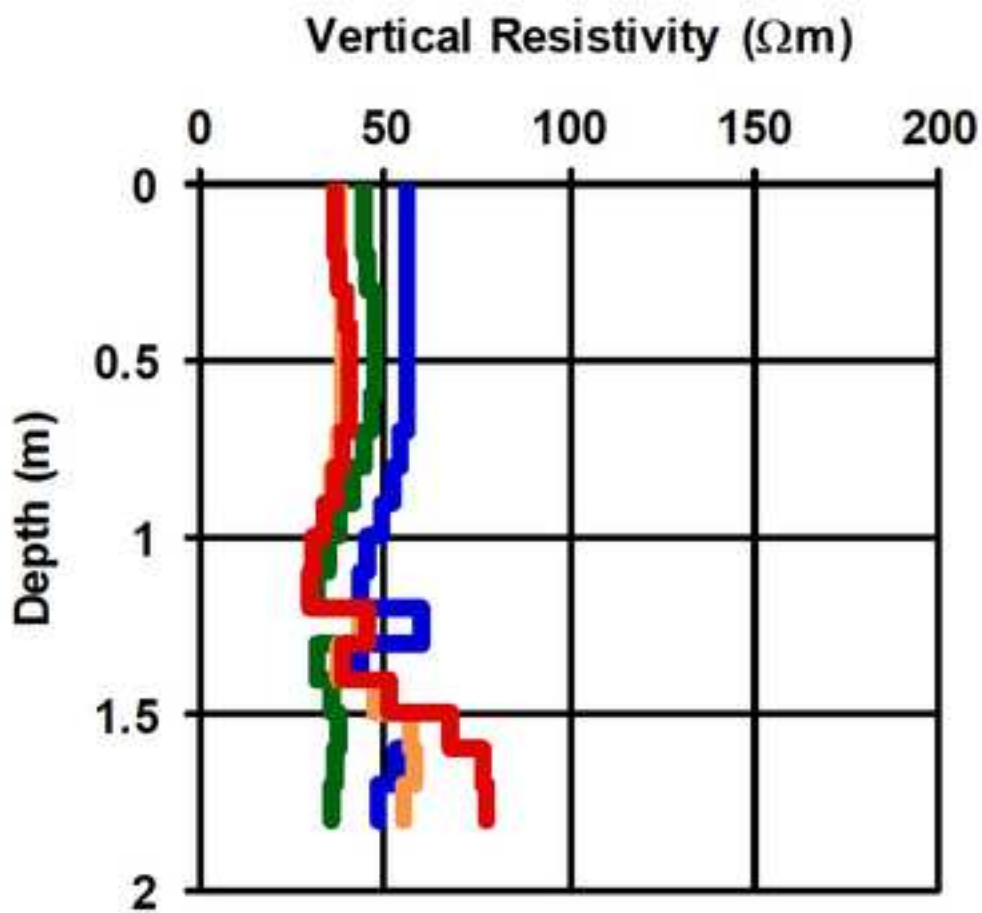
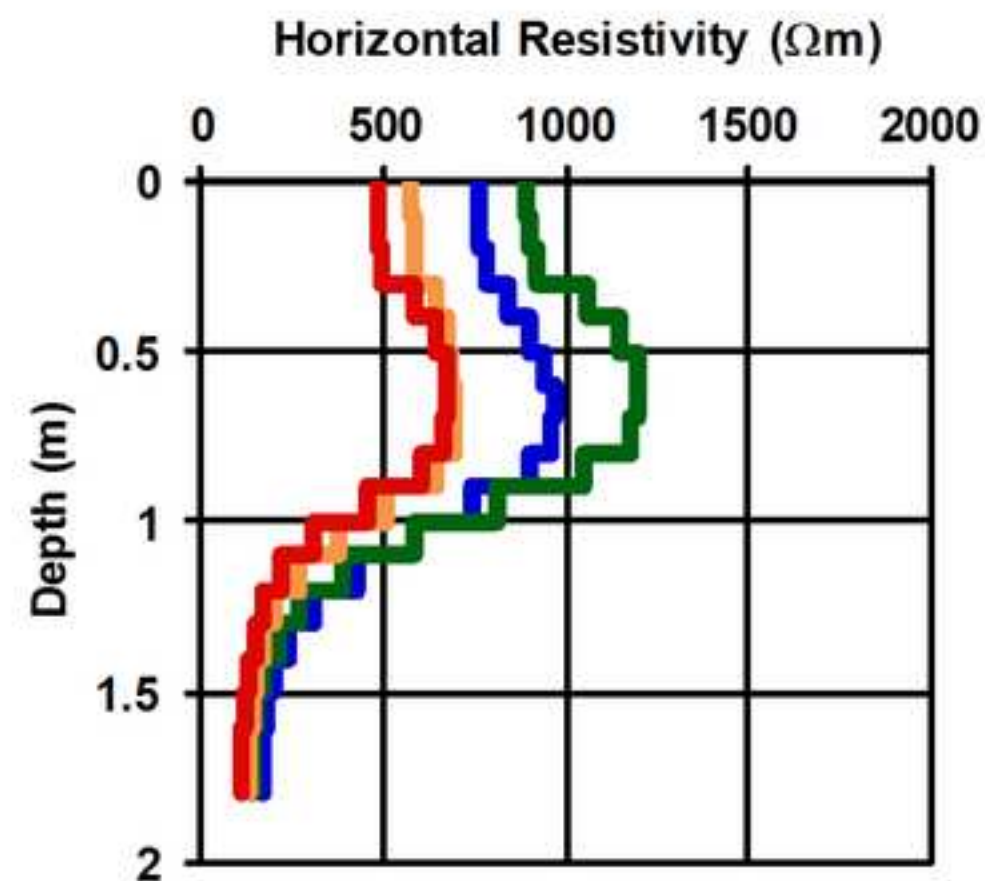
Figure(s)

[Click here to download high resolution image](#)



Figure(s)

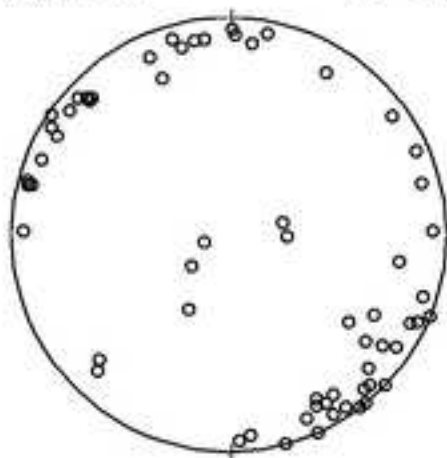
[Click here to download high resolution image](#)



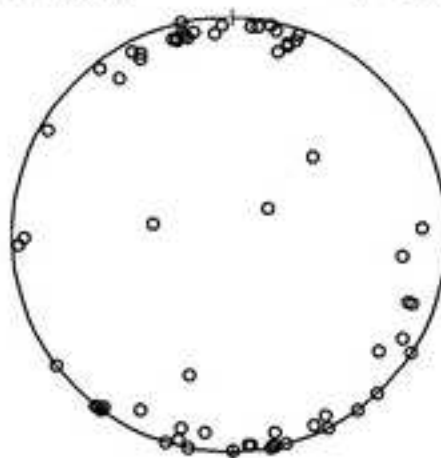
Figure(s)

[Click here to download high resolution image](#)

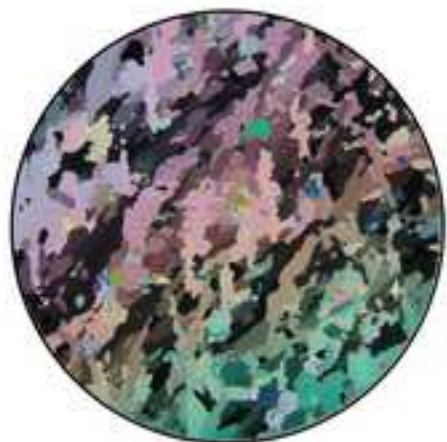
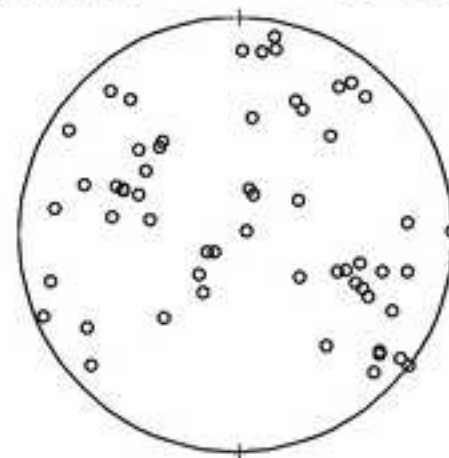
(a) 0.60 m $A = 0.23$



(b) 1.39 m $A = 0.14$

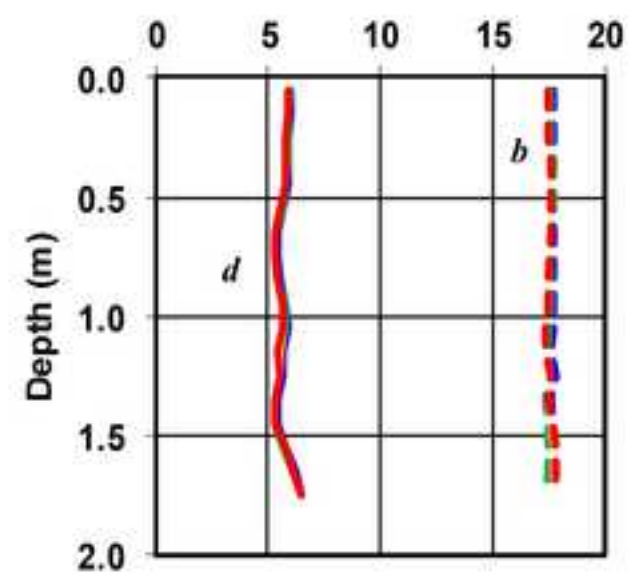
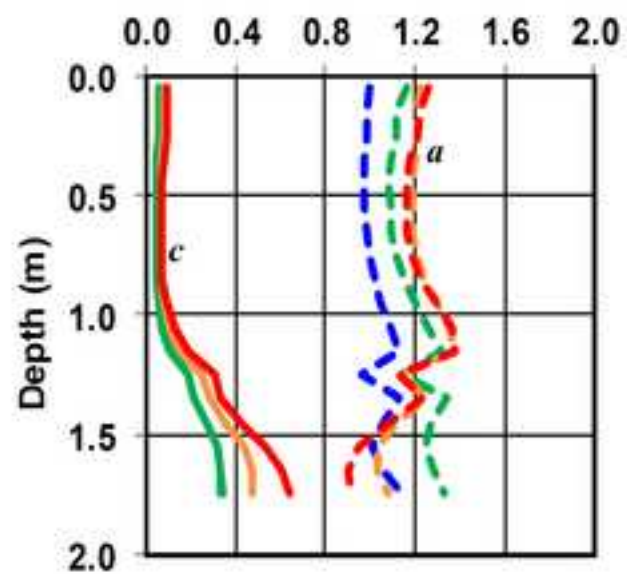
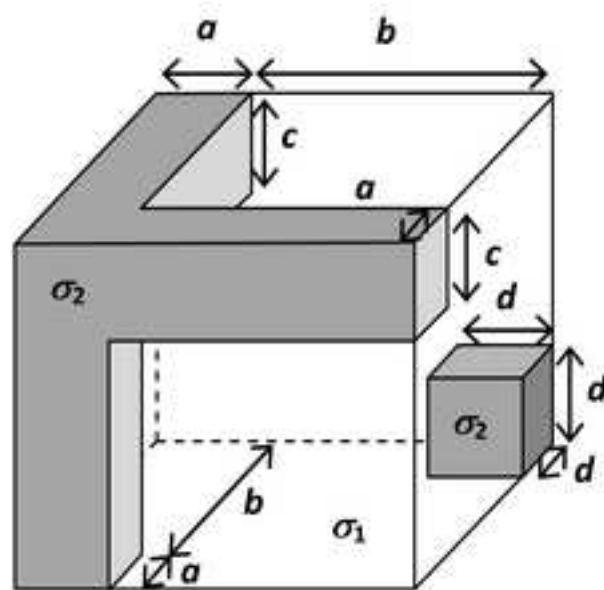


(c) 1.60 m $A = 0.67$



Figure(s)

[Click here to download high resolution image](#)



Figure(s)

[Click here to download high resolution image](#)

